Antarctic Science 36(5), 361–378 (2024) doi:10.1017/S0954102024000233

Permafrost and ground-ice conditions in the Untersee Oasis, Queen Maud Land, East Antarctica

DENIS LACELLE [1], MARJOLAINE VERRET[2], BENOIT FAUCHER [3], DAVID FISHER[4], ADAM GAUDREAU[1], ANDRÉ PELLERIN[5], MILES ECCLESTONE[6] and DALE T. ANDERSEN [7]

[1]*Department of Geography, Environment and Geomatics, University of Ottawa, Ottawa, ON, Canada*
[2]*Department of Arctic Geology, The University Centre in Svalbard, Longyearbyen, Svalbard and Jan Mayen, Norway*
[3]*Geological Survey of Canada, Ottawa, ON, Canada*
[4]*Department of Earth Sciences, University of Ottawa, Ottawa, ON, Canada*
[5]*Institute of Marine Sciences, University of Québec in Rimouski, Rimouski, QC, Canada*
[6]*School of the Environment, Trent University, Peterborough, ON, Canada*
[7]*Carl Sagan Center at the SETI Institute, Mountain View, CA, USA*
dlacelle@uottawa.ca

Abstract: Knowledge of Antarctic permafrost is mainly derived from the Antarctic Peninsula and Victoria Land. This study examines the 2019–2023 temperature and humidity conditions, distribution and development of polygonal terrain and the origin of ground ice in soils of the Untersee Oasis. In this region, the surface offset (MAAT ≅ MAGST) and the thermal offset (MAGST ≤ TTIT) reflect the lack of vegetation, absence of persistent snow and a dry soil above the ice table. The mean annual vapour pressure at the ground surface is approximately ~2× higher than in the air but is ~0.67× lower than at the ice table. The size of polygons appears to be in equilibrium with the ice-table depth, and numerical modelling suggests that the depth of the ice table is in turn in equilibrium with the ground surface temperature and humidity. The ground ice at the ice table probably originates from the partial evaporation of snowmelt that infiltrated the dry soil column. As such, the depth of the ice table in this region is set by the water vapour density gradient between the ground surface and the ice-bearing ground, but it is recharged periodically by evaporating snowmelt.

Key words: δD-$\delta^{18}O$, ground ice, ground temperatures, polygonal terrain, sublimation-type polygon

Introduction

Permafrost environments in ice-free areas of Antarctica range from small bedrock outcrops and nunataks to large oases situated in both coastal and inland regions of the continent (Vieira *et al.* 2010, Hrbáček *et al.* 2023). Despite being limited to a total area of ~55 000 km^2, or ~0.5% of the continent (Brooks *et al.* 2019), permafrost in ice-free regions is an important component of Antarctic terrestrial ecosystems as it influences pedologic, hydrologic, geomorphic and microbial processes (Levy *et al.* 2011, Guglielmin *et al.* 2014, Goordial *et al.* 2016, Faucher *et al.* 2017). However, knowledge of Antarctic permafrost remains largely limited to the two largest ice-free regions: the Antarctic Peninsula and the McMurdo Dry Valleys (MDVs) in Victoria Land. Table I lists acronyms and equations for permafrost-related terms used in the text.

Permafrost conditions in these two regions are related to air temperatures and the presence (or lack thereof) of vegetation and snow (Bockheim *et al.* 2007, Marchant & Head 2007, Adlam *et al.* 2010, Fountain *et al.* 2010, Levy *et al.* 2011). The Antarctic Peninsula has the warmest and wettest climate on the continent, with MAAT from near -5°C to -2°C (Bockheim *et al.* 2013) and total precipitations estimated at 500–2000 mm w.e. yr^{-1} in the western sector, but the latter is lower in the eastern sector (300–700 mm w.e. yr^{-1}; Schwerdtfeger 1984, Van Wessem *et al.* 2016). The presence of snow and vegetation in this region, and in a few others in Antarctica, results in a positive surface offset (MAGST > MAAT; i.e. Cannone & Guglielmin 2009, Hrbáček *et al.* 2023). The freeze-back of the active layer (40–200 cm) in winter results in a negative thermal offset (MAGST > TTOP) due to frozen soils having a higher thermal conductivity than when thawed (Vieira *et al.* 2010, Bockheim 2015, Hrbáček *et al.* 2023). The climate in the MDVs and other coastal sites in Victoria Land is much colder and drier, with MAAT ranging between -30°C and -15°C and total precipitation being < 50 mm w.e. yr^{-1} (Obryk *et al.* 2020). In this region, the thickness of the active layer varies between 90 cm near the coastal

Table I. List of acronyms and equations used in the text for various permafrost-related parameters.

Acronym	Meaning	Equation	Reference
MAAT	Mean annual air temperature	$\frac{It-If}{P}$	Smith & Riseborough (2002)
MAGST	Mean annual ground surface temperature	$\frac{nt\ It-nf\ If}{P}$	Smith & Riseborough (2002)
TITT	Mean annual temperature at the top of the ice table	$\frac{(rk\ nt\ It)-(nf\ If)}{P}$	Smith & Riseborough (2002)
Surface offset	Difference between MAGST and MAAT	$\frac{If(1-nf)}{P} - \frac{It(1-nt)}{P}$	Smith & Riseborough (2002)
Thermal offset	Difference between TTIT and MAGST	$\frac{ntIt(rk-1)}{P}$	Smith & Riseborough (2002)
FDDa (or If)	Freezing degree-days air	$\sum$ *mean daily air temperature* $< 0°C$	Smith & Riseborough (2002)
FDDs	Freezing degree-days surface	$\sum$ *mean daily surface temperature* $< 0°C$	Smith & Riseborough (2002)
TDDa (or It)	Thawing degree-days air	$\sum$ *mean daily air temperature* $> 0°C$	Smith & Riseborough (2002)
TDDs	Thawing degree-days surface	$\sum$ *mean daily surface temperature* $> 0°C$	Smith & Riseborough (2002)
Freezing n-factor	Ratio of ground surface freezing degree-days to air freezing degree-days	$\frac{FDDs}{FDDa}$	Smith & Riseborough (2002)
VEH	Vapour enhancement factor	$\frac{vapour\ pressure\ at\ surface}{vapour\ pressure\ in\ air}$	McKay *et al.* (2019)
Frost point n-factor	Ratio of ground surface frost point to air frost point (or ice table to ground surface)	$\frac{FPs}{FPa}$	

regions and 0 cm at the upper elevations (Hrbáček *et al.* 2023). The absence of vegetation and seasonal snow cover results in a surface offset near 0°C (MAGST ≈ MAAT; Lacelle *et al.* 2016). However, the thermal offset can be near 0°C in places with dry permafrost above the ice table (the interface between dry and icy permafrost; Lacelle *et al.* 2016, Lapalme *et al.* 2017b). Both regions host rock glaciers and solifluction features, ice-wedge polygons, thermokarst and gullies (Bockheim *et al.* 2013). However, sand-wedge and sublimation-type polygons occur only in the colder and drier upper elevations of the MDVs (Marchant & Head 2007). Ground ice is also present in both regions, with recent studies suggesting a widespread distribution of ice-rich permafrost (e.g. Lacelle *et al.* 2013, Lapalme *et al.* 2017a, Verret *et al.* 2021) and massive ice (Swanger *et al.* 2010, Swanger 2017, Gardner *et al.* 2022) in places previously classified as dry permafrost (Bockheim *et al.* 2007). Three main mechanisms of ground-ice emplacement have been proposed in Antarctic permafrost: 1) episodic freezing of snow meltwater, 2) diffusion of water vapour and 3) burial of glacial ice.

Despite the presence of several research stations in East Antarctica, long-term studies of permafrost conditions are mainly limited to the nunataks near the SANAE VI and Troll stations (Kotzé & Meiklejohn 2017, Hrbáček *et al.* 2021). Here, we provide the first report of permafrost conditions in the Untersee Oasis in Queen Maud Land, East Antarctica. The objectives of this study are to: 1) describe the temperature and humidity conditions of the air, ground surface and ice table and determine the surface and thermal offsets, the freezing n-factors and vapour enhancement factors, 2) describe the distribution of the polygonal terrain and characterize its morphology and depth to the ice table, 3) determine the origin of the ground ice at the ice table of the polygonal terrain and 4) describe the occurrence of the early-stage development of sublimation-type polygons. The permafrost conditions from the Untersee Oasis are compared to those from nearby Schirmacher Oasis and the MDVs.

Study area

The Untersee Oasis (71.3°S, 13.5°E) is located in the Gruber Mountains of Queen Maud Land, ~150 km from the coast and ~90 km south-east of the Schirmacher Oasis (Fig. 1). The Untersee Oasis has a surface area of 238 km^2 and is surrounded by the East Antarctic Ice Sheet. The permafrost environment in the ice-free terrain occupies 95 km^2 and includes three main ice-free regions: 1) the terrain surrounding Lake Untersee, a ~11 km-long and ~4 km-wide north-south-trending valley, 2) Aurkjosen Cirque, a ~3.5 km-long and ~2 km-wide east-west-trending valley with a small hanging glacier, and 3) Pritzker Valley (informal name), a 2.5 km-long and 0.5 km-wide north-east-south-west-trending valley with a small ice patch near the head of the valley.

The local geology in the oasis consists of Precambrian norite, anorthosite and anorthosite-norite alternation of the Eliseev massif complex (Kampf & Stakerbrandt 1985, Bormann *et al.* 1986, Paech & Stackebrandt 1995). The East Antarctic Ice Sheet covered the Untersee Oasis during the Late Pleistocene. Based on ^{14}C ages of stomach oils from snow petrel nests, thinning of the ice sheet began at *c.* 35–30 ka, which led to a reconfiguration of the local ice flow (Hiller *et al.* 1988). The Untersee Oasis came to its current configuration at

https://doi.org/10.1017/S0954102024000233 Published online by Cambridge University Press

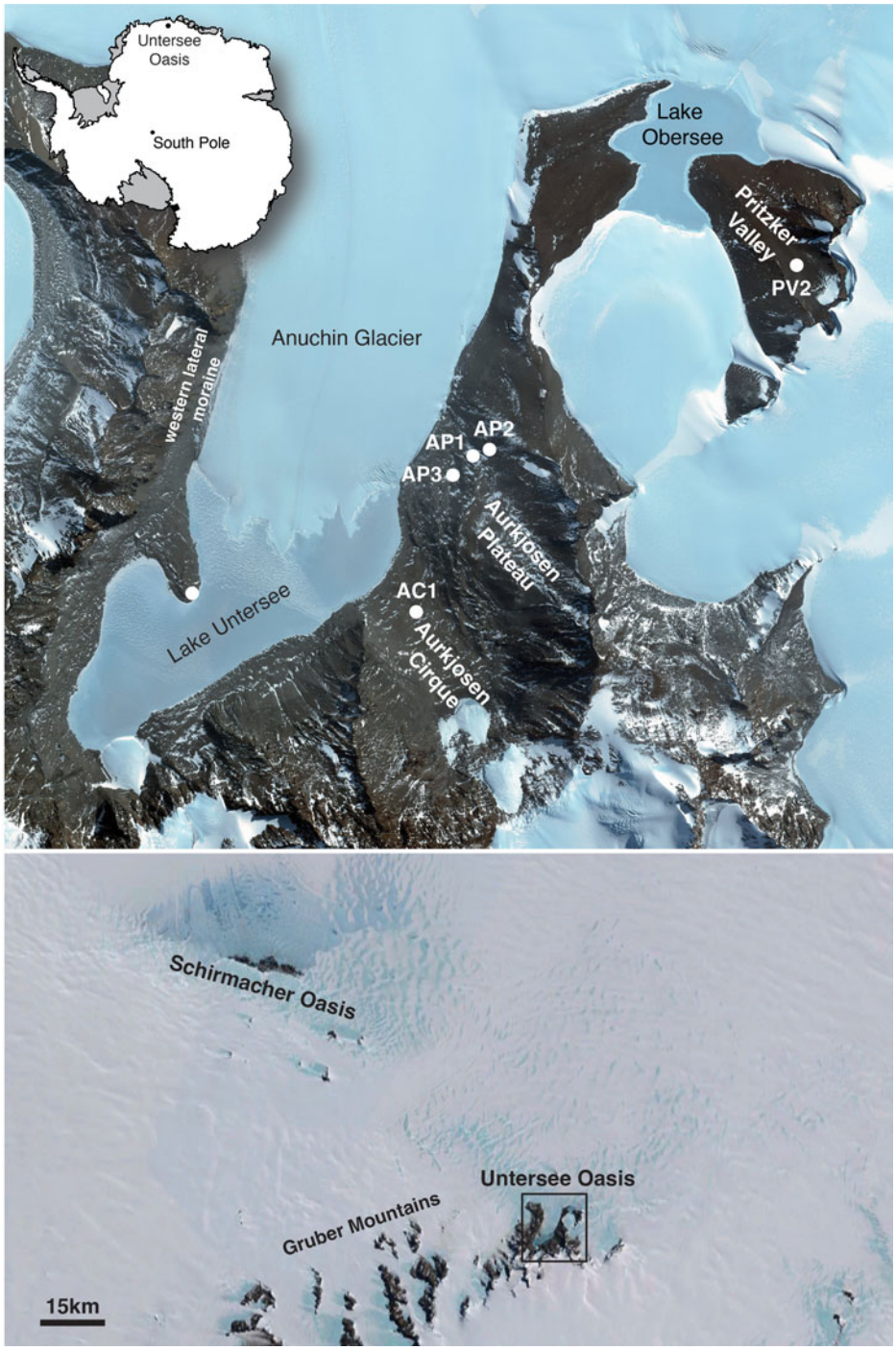

Figure 1. Location of sites in the Untersee Oasis, Queen Maud Land, Antarctica. Background Digital Globe NextView satellite imagery, 7 December 2017; ©2020 Digital Globe NextView License (provided by NGA commercial imagery program).

c. 6–4 ka. The surface sediments consist mainly of till and colluvium, often covered by a thin layer of aeolian sediments (Schwab 1998). Vegetation and lichens are absent, and the soils consist of poorly sorted sediments with low organic matter content (Shamilishvili *et al.* 2020). However, hypolithic microbial communities can be observed under some quartz rocks.

The region is characterized as a polar desert climate regime. The only long-term climate record in the region comes from Novolazarevskaya Station in the Schirmacher Oasis (herein referred as Novo; 70.78°S, 11.84°E; 120 m above sea level (a.s.l.); https://gtnp.arcticportal.org/). At Novo, the MAAT for the 1962–2022 period is -10.2°C ± 0.6°C. Air temperatures showed a significant

https://doi.org/10.1017/S0954102024000233 Published online by Cambridge University Press

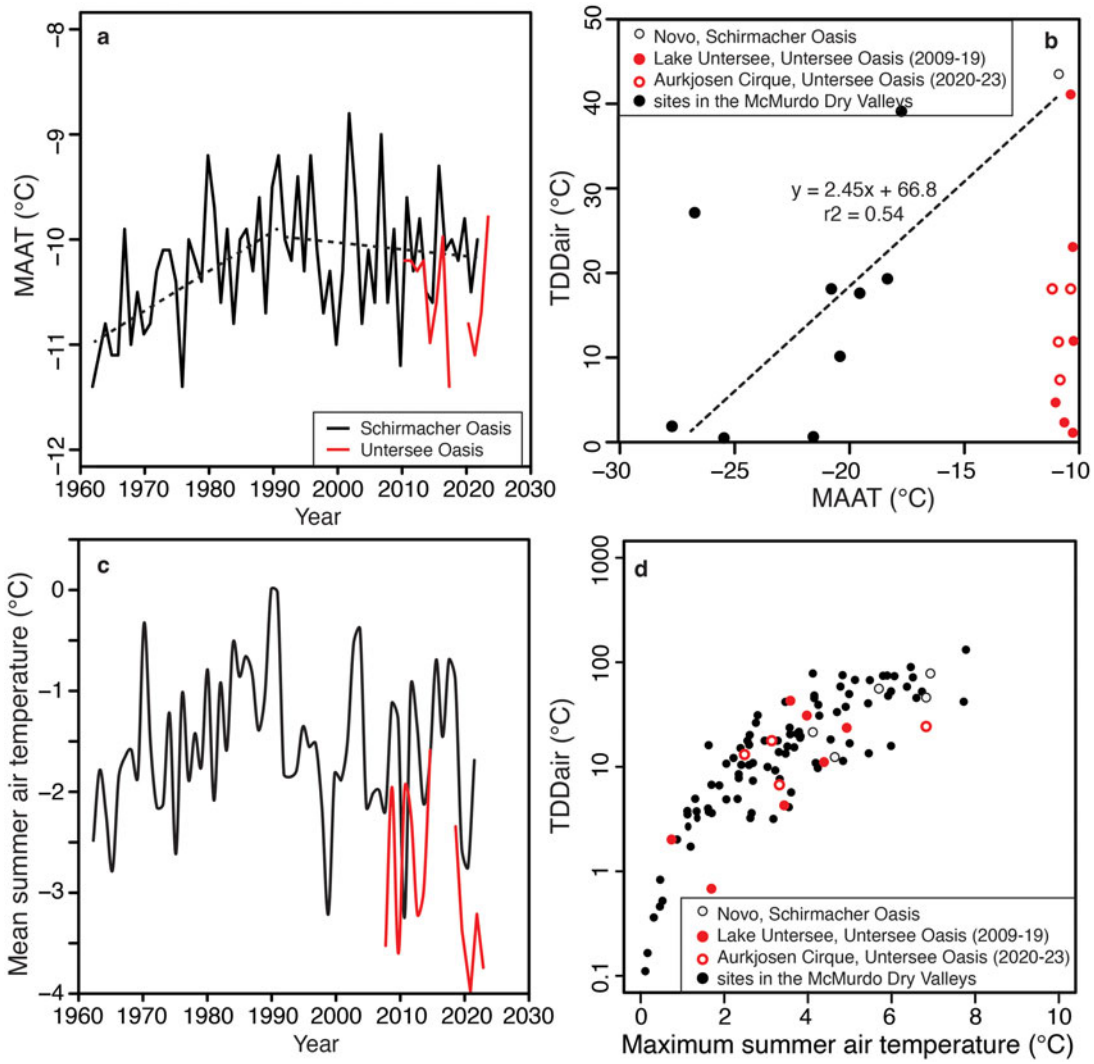

Figure 2. a. 1960–2023 mean annual air temperature (MAAT) in the Untersee Oasis and the Schirmacher Oasis, Queen Maud Land, Antarctica. **b.** Comparison of thaw degree-days in the air (TDDa) and MAAT in the Untersee Oasis, the Schirmacher Oasis and the McMurdo Dry Valleys. **c.** 1960–2023 mean summer air temperatures in the Untersee Oasis and the Schirmacher Oasis. **d.** Thaw degree-days in the air (TDDa) *vs* mean summer air temperature in the Untersee Oasis compared to those in the Schirmacher Oasis and the McMurdo Dry Valleys.

warming trend until 1991 (0.044°C yr^{-1}), largely due to increasing summer air temperatures (+0.056°C yr^{-1} for 1962 to 1991), followed by a non-significant cooling trend from 1992 to 2022 (-0.0038°C yr^{-1}; Fig. 2a). In the Untersee Oasis, meteorological data were collected during the 2008–2017 period by an automated weather station along the shoreline of Lake Untersee (71.34335°S, 13.46024°E, 612 m a.s.l.; Andersen *et al.* 2015). This station was damaged by a glacial lake outburst flood in early 2019 (i.e. Faucher *et al.* 2021), and a new station was installed in late 2019 in adjacent Aurkjosen Cirque (71.34488°S, 13.55587°E, 660 m a.s.l.). Based on these two stations, the MAAT in the Untersee Oasis for the 2008–2022 period is -10.6°C ± 0.4°C, ~0.5°C cooler than at Novo (Fig. 2a). The lower MAAT in the Untersee Oasis is attributed to cooler summers, which are ~0.9°C cooler than at Novo (Fig. 2b). This also results in the thaw degree-days at the Untersee Oasis (ranging from 5 to 41) being substantially lower than at Novo (Fig. 2c,d). The Untersee Oasis has a mean relative humidity of 42% ± 5%. Wind speeds average 5.4 m s^{-1}, but wind can gust up to 42 m s^{-1}. Despite having a relatively high MAAT for Antarctica, the climate in the Untersee Oasis is dominated by intense wind-driven ablation, limiting surface melt due to the cooling associated with the latent heat of evaporation and sublimation (e.g. van den Broeke *et al.* 2006, Hoffman *et al.* 2008). There are no gullies along the valley slopes. The only evidence of surface melt comes from observations of wetting of the uppermost 2–3 cm of the soils and the presence of

https://doi.org/10.1017/S0954102024000233 Published online by Cambridge University Press

Table II. Location of meteorological stations in the Untersee Oasis, Queen Maud Land, Antarctica, and summary of main parameters.

Parameter	Aurkjosen Cirque	Aurkjosen Plateau		Pritzker Valley
Acronym	AC1	AP1, AP2	AP3	PV2
Latitude	-71.34488	-71.31762°	-71.33168	-71.29252
Longitude	13.55587	13.58179°	13.58011	13.69651
Elevation (m)	660	1015	1002	1035
Period	2020–2023	2019–2020	2022–2023	2022–2023
Ice-table depth (cm)	n.d.	39	n.d.	80
MAAT (°C)	-10.5 ± 0.4	-	-	-
MAGST (°C)	-10.0 ± 0.3	-14.2	-	-11.8
TTIT (°C)	-	-13.3	-	-11.7
Surface offset	0.4	n.d.	n.d.	n.d.
Thermal offset	n.d.	0.9	n.d.	0.1
RH air ($\%_{ice}$)	30.3	-	-	-
RH surface ($\%_{ice}$)	-	81.1	-	77.2
RH ice table ($\%_{ice}$)	-	100	-	100
Frost point air (°C)	-20.0	-	-	-
Frost point surface (°C)	-	-16.8	-	-15.4
Frost point ice table (°C)	-	-13.1	-	-11.7

RH = relative humidity.

evaporative calcite crusts on the surface of clasts in the vicinity of residual snow patches (Lacelle *et al.* 2024).

There has been no report of the permafrost conditions in the Untersee Oasis. However, in the nearby Schirmacher Oasis, ground temperatures have been monitored since 2008 as part of the Circumpolar Active Layer Monitoring (CALM) programme (https://gtnp.arcticportal.org/). At Novo, the thickness of the active layer varies annually from 67 to 92 cm, the surface offset averages 1.0°C ± 1.5°C and the thermal offset is near 0°C (0.4°C ± 1.1°C; Hrbáček *et al.* 2023). Modelling estimated the mean annual temperature at the top of the permafrost to be within the range of -8°C to -10°C (Obu *et al.* 2020).

Methodology

Ground temperature and humidity measurements

The meteorological station on the valley floor of Aurkjosen Cirque (AC1, 660 m a.s.l.) is equipped with Onset HOBO U23 ProV2 sensors to monitor temperatures in the air and at the soil surface (accuracy ±0.2°C). The valley floor of Aurkjosen Cirque was too stony to install soil sensors. As such, we installed smaller stations on the Aurkjosen Plateau: two stations were installed ~500 m apart in December 2019 (AP1, 1015 m a.s.l.; AP2, 1045 m a.s.l.), but due to some sensor failures at AP1 and AP2 in 2019–2020, a third station was installed in November 2022 (AP3, 1002 m a.s.l.; Fig. 1). In Pritzker Valley, three stations were installed in November 2021; however, only one of them recorded measurements for > 1 month (PV2, 1035 m a.s.l.; Fig. 1). These smaller stations all consist of an Onset 4 channel smart logger (U12-008) equipped with three U23 Pro v2 temperature and relative humidity sensors: 1 m above the surface, at the soil surface (covered with a thin layer of soil to ensure that the surface albedo was maintained) and at the ice table. The placement of the sensors aimed to minimally disturb the soil and ensure optimal thermal connectivity with the soil. All loggers recorded measurements at hourly intervals, from which mean daily values were calculated. The accuracy of the relative humidity sensors is ±2.5% in the 10–90% range and ±5% at < 10% or > 90%. The relative humidity measurements are recorded with respect to liquid water (RH_w) but were corrected to relative humidity with respect to ice (RH_{ice}) using the temperature-dependent ratio of the saturation vapour pressure over ice and water (i.e. Hagedorn *et al.* 2007, Andersen *et al.* 2015). The mean daily frost point temperatures of the air, ground surface and ice table were then calculated based on the mean daily vapour pressure and the saturation vapour pressure curve relative to ice. Table II provides details of the meteorological stations in the Untersee Oasis.

The air and ground temperature measurements were used to quantify the surface offset and the thermal offset (Table I; Smith & Riseborough 1996, Eaton *et al.* 2001, Smith & Riseborough 2002). The monthly variations in freezing n-factors (Table I) allowed us to investigate the sub-seasonal changes in air and ground temperature relations (Klene *et al.* 2001, Karunaratne & Burn 2004). Additionally, the stability of the ice table beneath dry permafrost was assessed from the vapour enhancement factor (McKay *et al.* 2019) and from the mean monthly variations of the frost point n-factors (Table I).

https://doi.org/10.1017/S0954102024000233 Published online by Cambridge University Press

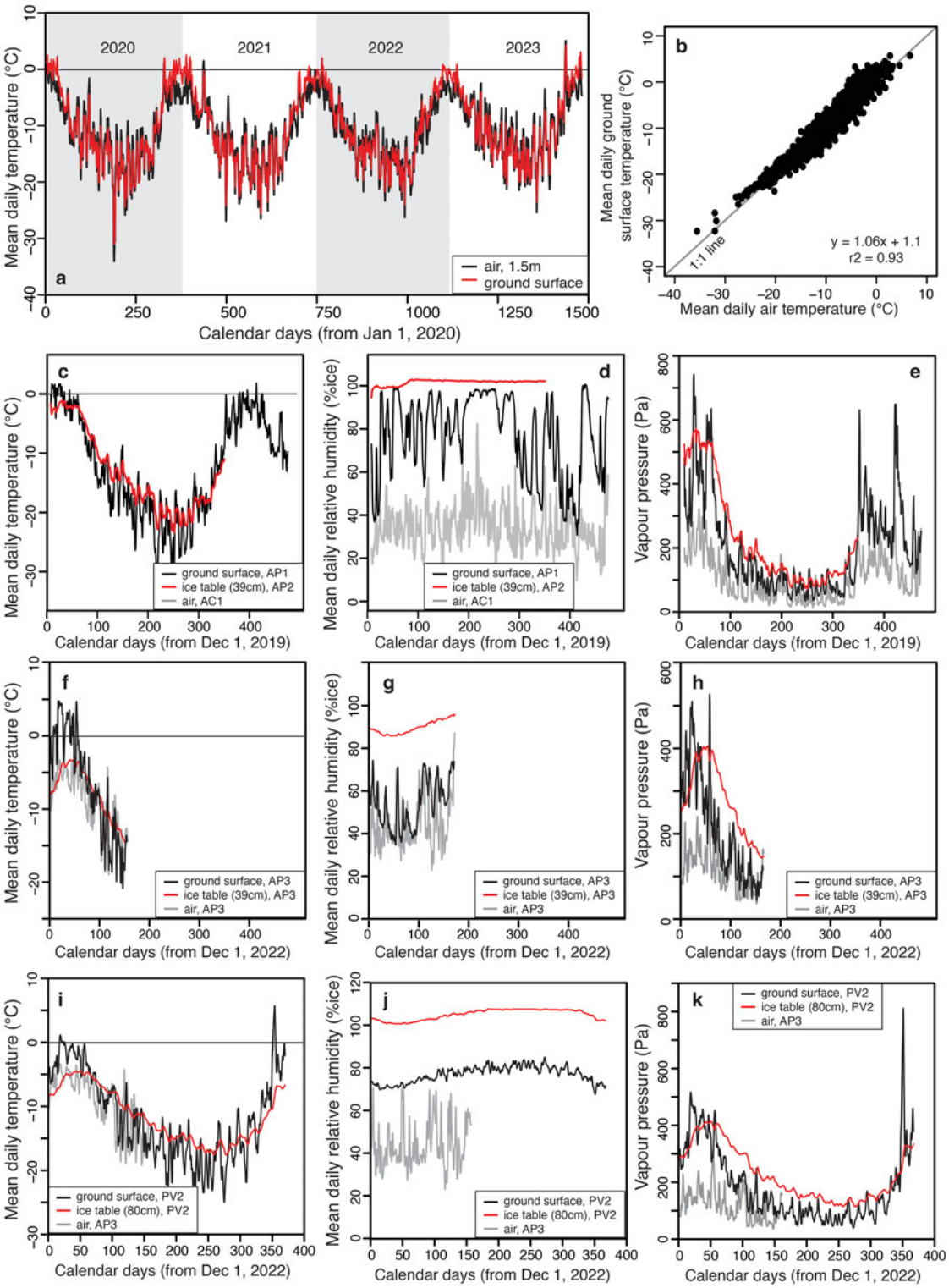

Figure 3. Mean daily temperatures and humidity in the air, ground surface and ice table at various sites in the Untersee Oasis, Queen Maud Land, Antarctica. **a.** 1 December 2020 to 31 December 2023 mean daily temperatures in Aurkjosen Cirque (AC1). **b.** Comparison of mean daily ground surface temperature and mean daily air temperature in Aurkjosen Cirque. 1 December 2019 to 10 March 2021 **c.** mean daily temperatures, **d.** relative humidity and **e.** vapour pressure in Aurkjosen Plateau (AP1, AP2). 1 December 2022 to 12 May 2023 **f.** mean daily temperatures, **g.** relative humidity and **h.** vapour pressure in Aurkjosen Plateau (AP3). 1 December 2022 to 5 December 2023 **i.** mean daily temperatures, **j.** relative humidity and **k.** vapour pressure in Pritzker Valley (PV2).

https://doi.org/10.1017/S0954102024000233 Published online by Cambridge University Press

The thermal diffusivity (D) is a measure that is difficult to accurately calculate as it is dependent on soil properties (grain size, mineralogy, density, moisture and phase changes). Here, we used a finite difference method based on the heat equation (equation 3 in Pringle *et al.* 2003; and appendix A in Marinova *et al.* 2022) to approximate the apparent thermal diffusivity of the soil column from the mean daily ground temperatures at the ground surface and ice table and solving the time derivative and second-order space derivative in the heat conduction equation at each time step.

Polygonal terrain and ice-table depths

In the Untersee Oasis, polygonal terrain was observed in two regions: 1) Pritzker Valley and 2) along the west lateral moraine of the Anuchin Glacier (Fig. 1). The polygons in Pritzker Valley are well-defined and were digitized in *ArcGIS10* using 50 cm-resolution DigiGlobe satellite imagery (13 September 2021). The polygons along the west lateral moraine of the Anuchin Glacier are not as well defined as those in Pritzker Valley. As such, their morphometric characteristics were determined from photographs acquired in December 2017 and November 2019 using a DJI Phantom 4 Pro unmanned aerial vehicle (e.g. Faucher *et al.* 2021a). The unmanned aerial vehicle was flown 30 m above the ground surface in a gridded survey using the *DJI Mission Planner* software with 85% forward and 75% side overlap. The photographs at 1 cm resolution were captured at 400 ISO, with a shutter speed of 1/1000 s and focus fixed at infinity. The accuracy of the Global Positioning System (GPS) tags from the JPEG Exif metadata was optimized with ground control points surveyed using a Trimble R9s differential GPS (dGPS) and a local base station. *Agisoft Photoscan Pro* v.1.4 software was used to generate point cloud models of the area. The dense point cloud models in .LAS data format (WGS 84 UTM zone 33S projection) were used to create orthomosaics, from which polygonal terrain measurements were derived.

As a relation between polygon diameter and ice-table depth was observed at the high elevations of the MDVs (Mellon *et al.* 2014), we quantified both parameters at some sites to determine whether such a relation exists in Pritzker Valley and along the west lateral moraine of the Anuchin Glacier. The depth to the ice table was determined during the first week of December 2021 by digging soil pits in the centre of polygons of different diameters (10–70 m). The reported depths are based on the average of three to five measurements in each polygon.

δD-$\delta^{18}O$ composition of ground ice at the ice table

Where possible, samples at the ice table in Pritzker Valley were collected and analysed for δD-$\delta^{18}O$ to infer the source of water recharging the ground ice. The $^{18}O/^{16}O$ and D/H ratios of the melted ice samples were determined using a Los Gatos Research liquid water analyser coupled to a CTC LC-PAL autosampler for simultaneous $^{18}O/^{16}O$ and D/H ratio measurements of H_2O and verified for spectral interference contamination. The results are presented using the δ-notation ($\delta^{18}O$ and δD), where δ represents the parts per thousand differences for $^{18}O/^{16}O$ or D/H in a sample with respect to Vienna Standard Mean Ocean Water (VSMOW). Analytical reproducibility values for $\delta^{18}O$ and δD are ±0.3‰ and ±1‰, respectively.

Results

Air and ground surface temperatures in Aurkjosen Cirque

The 1 December 2020 to 31 December 2023 mean daily air and ground surface temperatures recorded on the valley floor of Aurkjosen Cirque (AC1) are shown in Fig. 3a. The mean daily temperatures vary between -35°C and +7°C, and the ground surface and air temperatures are highly correlated (Fig. 3b). Annually, the MAAT (-10.5°C ± 0.4°C) and MAGST (-10.0°C ± 0.3°C) are similar, providing a surface offset of +0.5°C ± 0.1°C. Seasonally, the temperatures at the ground surface are 2–7°C warmer in summer than in the air due to solar heating. This is illustrated in the monthly freezing *nf*, where values are < 1 between November and February (0.60–0.03). Between March and October, the freezing *nf* values are > 1 (1.00–1.06), indicating that the ground surface temperatures are slightly cooler than the air. With a mean relative humidity of 30.3%, the mean annual frost point of the air is -20.0°C.

Ground temperature and humidity conditions on the Aurkjosen Plateau. Figure 3c–e shows the 2019–2020 mean daily temperatures and relative humidity values at the ground surface (AP1) and ice table (AP2) measured on the Aurkjosen Plateau. As both stations are close to each other (~500 m distance), we assume that the temperature and relative humidity conditions are similar at both sites. The active layer (depth of 0°C isotherm) reaches a thickness of 25 cm, and the ice table is at a depth of 39 cm. The MAGST is -14.2°C ± 8.2°C and the mean annual temperature at the ice table is -13.3°C ± 6.7°C (thermal offset of 0.8°C). The apparent thermal diffusivity of the dry soil is constant throughout the year (4.5×10^{-6} m^2 s^{-1}), as expected if the soils remain relatively dry year round. The mean annual relative humidity is 81.1 ± 16%$_{ice}$ at the ground surface and is saturated at the ice table (100%$_{ice}$). At the ground surface, the relative humidity is lower in summer and approaches near 100%$_{ice}$ in winter. The mean annual

https://doi.org/10.1017/S0954102024000233 Published online by Cambridge University Press

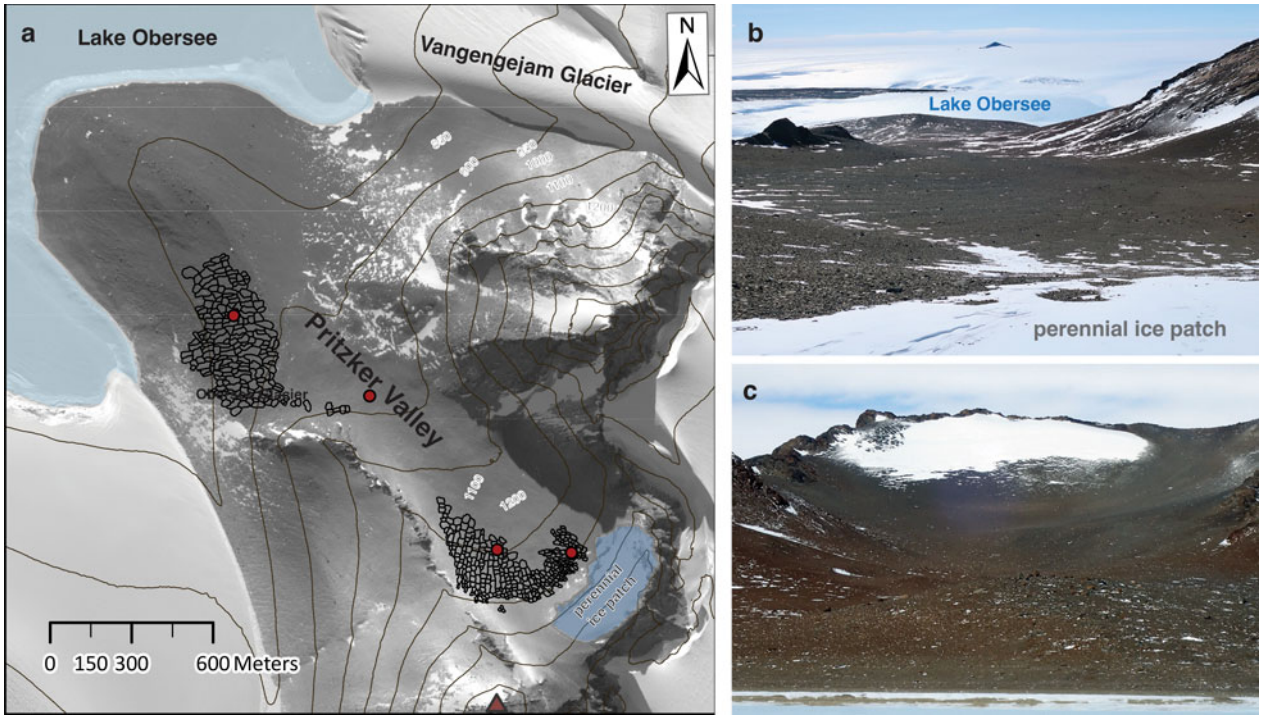

Figure 4. a. Map showing the distribution of polygonal terrain in Pritzker Valley, Untersee Oasis. **b. & c.** Field photographs (December 2021) of Pritzker Valley.

frost points for the ground surface and ice table are -16.8°C and -13.1°C, respectively.

Station AP3 recorded the temperature and relative humidity values of the air, ground surface and ice table (40 cm) for approximately half a year (23 November 2022 to 12 May 2023; Fig. 3f–h). The mean daily air and ground surface temperatures vary between -21°C and +5°C and are highly correlated (ground surface = 1.55(air) + 7.6; $r^2 = 0.85$). Seasonally, the temperatures at the ground surface are up to 10°C warmer in summer due to solar heating. The summer relative humidity is 48.8 ± 9.4%$_{ice}$ at the ground surface and is near 100%$_{ice}$ at the ice table.

Ground temperature and humidity conditions in Pritzer Valley

Station PV2 recorded the temperature and humidity values at the ground surface and ice table for 1 December 2022 to 5 December 2023. The sensor in the air failed after a few days; thus, we instead used the air measurements from the Aurkjosen Cirque Plateau (AP3), located nearby and at a similar elevation (Fig. 3i–k). The air and ground surface temperatures are highly correlated (ground surface = 1.17(air) + 3.1; $r^2 = 0.88$). Except for an anomalously warm 2 days in late 2023, there is no active layer at the site, and dry permafrost extends to the ground surface. Annually, the MAGST (-11.8°C ± 6.8°C) and TTIT (-11.7°C ± 4.2°C) are similar, providing a thermal offset of 0.1°C. Seasonally, the temperatures at the ground surface are 2–5°C warmer in summer than those in the air, but they are more similar in winter. The apparent thermal diffusivity also remains constant throughout the year, with the diffusivity being only 1% higher in winter (8.55×10^{-6} m^2 s^{-1}) than during the summer (8.48×10^{-6} m^2 s^{-1}). The mean annual relative humidity is 77.2 ± 3.8%$_{ice}$ at the ground surface (with lower values in summer) but remains near saturation at the ice table. The mean annual frost points for the ground surface and ice table are -15.4°C and -11.7°C, respectively.

Polygonal terrain in the Untersee Oasis

In Pritzker Valley, field observations and the high-resolution satellite images show little variation in the morphology of polygons: they all exhibit flat centres and shallow troughs (~5–10 cm deep and ~25–50 cm wide). Trough intersections are predominately triple junctions. The diameter of polygons ranges from 10 to 70 m ($n = 543$), and a general increase in polygon size as a function of increasing distance to the local ice patch at the head of the valley is observed (Fig. 4). The nature of these polygons (ice wedge or sand wedge) is unknown. The ground ice at the ice table in the centre of two polygons in Pritzker Valley has high $\delta^{18}O$ values (-9.8‰ at 68 cm ice-table depth and -7.3‰ at 58 cm ice-table

https://doi.org/10.1017/S0954102024000233 Published online by Cambridge University Press

Figure 5. a.–c. Field photographs of the polygonal terrain developing over buried glacial ice along the western lateral moraine of the Anuchin Glacier in the Untersee Oasis. **d. & e.** Field photographs showing the development of sublimation-type sand-wedge polygons.

depth) and very low the D-excess values (-91.4‰ and -105.8‰, respectively).

Along the western lateral moraine of the Anuchin Glacier, sand-wedge polygons are developing in the buried glacial ice (Fig. 5). The polygons all have flat centres and narrow/shallow troughs (< 5 cm deep and < 10 cm wide). The polygons closer to the Anuchin Glacier have smaller diameters (9–13 m; $n = 7$) and thinner sediment accumulation over the ice (< 5 cm), whereas those farther away from the glacier have larger

https://doi.org/10.1017/S0954102024000233 Published online by Cambridge University Press

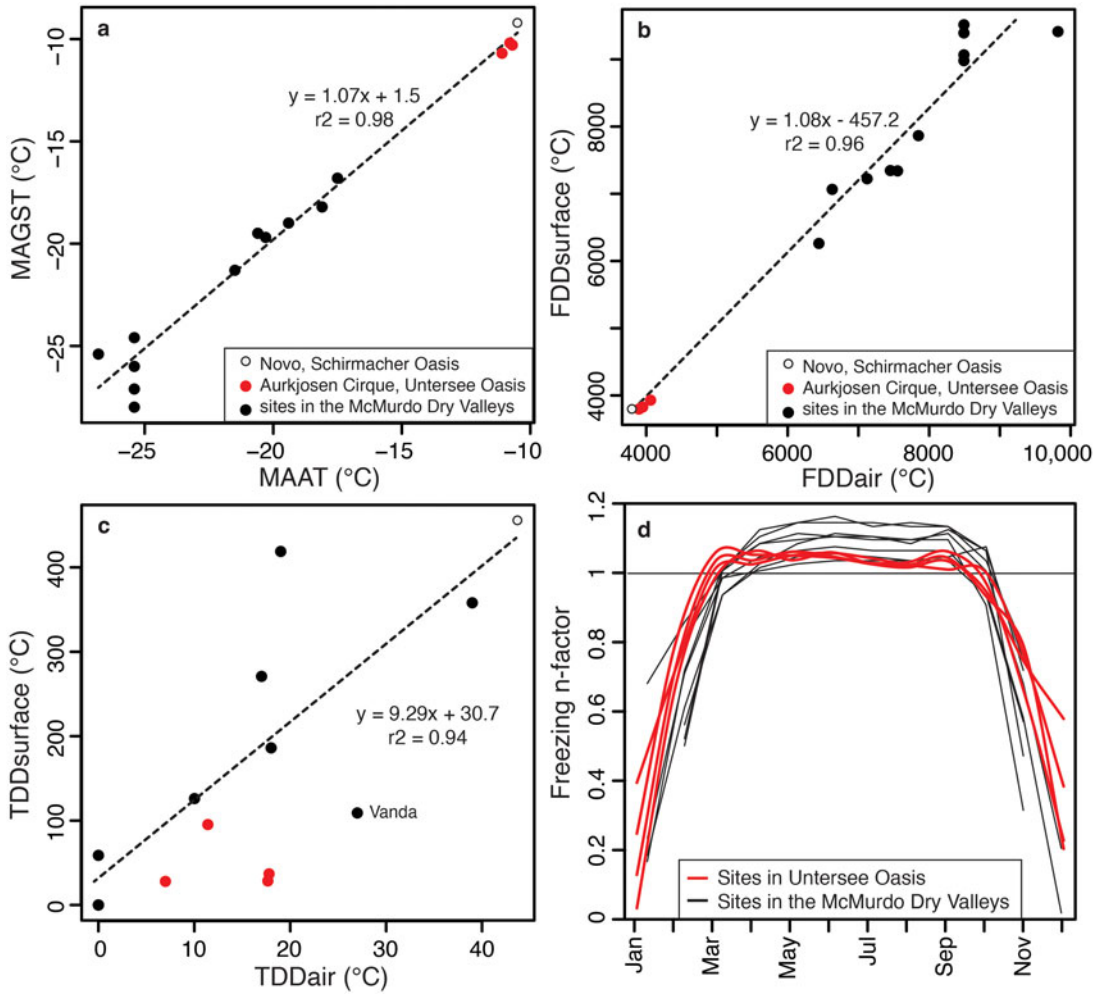

Figure 6. Air and ground surface temperature relations for sites in the Untersee Oasis compared to the Schirmacher Oasis and sites McMurdo Dry Valleys. **a.** Diagram showing the relation between mean annual air temperature (MAAT) and mean annual ground surface temperature (MAGST) for each of the stations. **b.** Comparison of freezing degree-days in the air (FDDa) and freezing degree-days surface (FDDs). **c.** Comparison of thaw degree-days in the air (TDDa) and thaw degree-days surface (TDDs). **d.** Comparison of monthly freezing n-factors.

diameters (10–18 m; $n = 10$) and a thicker accumulation of sediments (> 10 cm).

Discussion

Ground thermal and humidity conditions in the Untersee Oasis

Together, the data from the four sites illustrate the general ground thermal and humidity conditions in the Untersee Oasis. For the 2019–2023 period, the MAGST (-10.0°C ± 0.3°C) approximates the MAAT (-10.5°C ± 0.4°C), giving a surface offset of +0.5°C (Fig. 3b). Surface offsets near 0°C were also observed at Novo and various sites in the MDVs (Fig. 6a), and they are caused by the absence of vegetation and seasonal snow cover at the sites (Lacelle *et al.* 2016). The FDDa values in the Untersee Oasis are in the range of those at Novo (approximately -4000), and like the sites in the MDVs, the FDDa approximates the FDDs (Fig. 6b). However, the TDDa at Untersee Oasis (5–20) are substantially lower than at nearby Novo (42) but are in the range of those in the stable upland zone of the MDVs (Fig. 6c). At Novo and most sites in the MDV, TDDs is ~9–10× higher than the TDDa; however, in the Untersee Oasis, the TDDs are only 2–5× greater than the TDDa (Fig. 6c). Therefore, in terms of a comparison between MAAT and MAGST, the Untersee Oasis more closely resembles Novo and is warmer than at any sites in the MDVs. However, with TDDa of < 20 and TDDs of < 100, the summer condition in the Untersee Oasis is more like the high-elevation sites in the stable upland zone of the MDVs. As such, despite having similar ground surface conditions (absence of vegetation and

https://doi.org/10.1017/S0954102024000233 Published online by Cambridge University Press

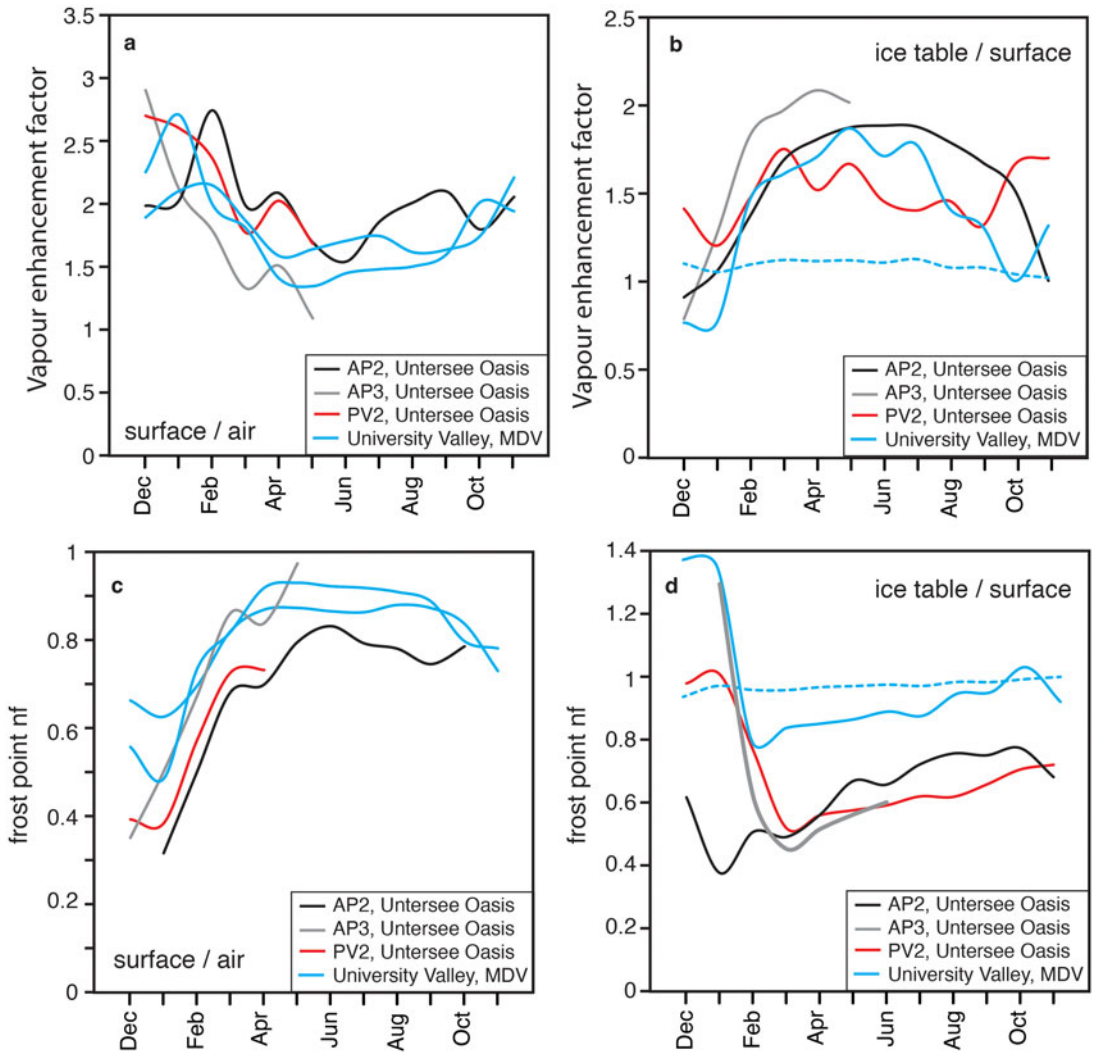

Figure 7. Vapour enhancement factor **a.** between the ground surface and air and **b.** between the ice table and ground surface. Frost point n-factor **c.** between the ground surface and air and **d.** between the ice table and ground surface. Data used for calculations for University Valley are from Lacelle *et al.* (2016) and Marinova *et al.* (2022). MDV = McMurdo Dry Valleys.

snow), a process (e.g. ablation) must be affecting the surface energy balance during the summer in the Untersee Oasis and causing the ground surface to be cooler than at other sites with similar TDDa.

In the Untersee Oasis, the TTIT is slightly higher than the MAGST (thermal offset +0.1°C to +0.9°C). A positive thermal offset was also observed in other regions in Antarctica (Hrbáček *et al.* 2023) and was suggested to be caused by the soil being mainly dry year round (no seasonal change in the soil thermal conductivity due to the absence of a liquid-ice phase change in the active layer; Lacelle *et al.* 2016). The thermal offset is negative where the active layer experiences seasonal freezing and thawing (the thermal conductivity of frozen soils is greater than for thawed soils, which results in a negative thermal offset; Table I; i.e. Smith & Riseborough 1996, Smith & Riseborough 2002).

At the Untersee Oasis, the relative humidity at the ground surface is consistently higher than in the air, and this is also the case when the measurements are converted to vapour pressure (Fig. 3). In fact, the mean annual vapour enhancement factor between the ground surface and the air averages 2.0 on the Aurkjosen Plateau; the same calculation using the data from two sites in University Valley in the MDVs provides values of 1.9 and 1.6 (Fig. 7a,b). In Pritzker Valley, the mean summer vapour enhancement factor (2.6) is similar to that on the Aurkjosen Plateau (2.3), as well as those in University Valley (2.1 and 2.3). Therefore, despite the MAAT approximating the MAGST at all of these sites, the mean annual vapour pressure at the ground surface is higher by a factor of ~2 relative to that of the air. A few hypotheses have been advanced to explain the greater moisture at the ground surface relative to that in

https://doi.org/10.1017/S0954102024000233 Published online by Cambridge University Press

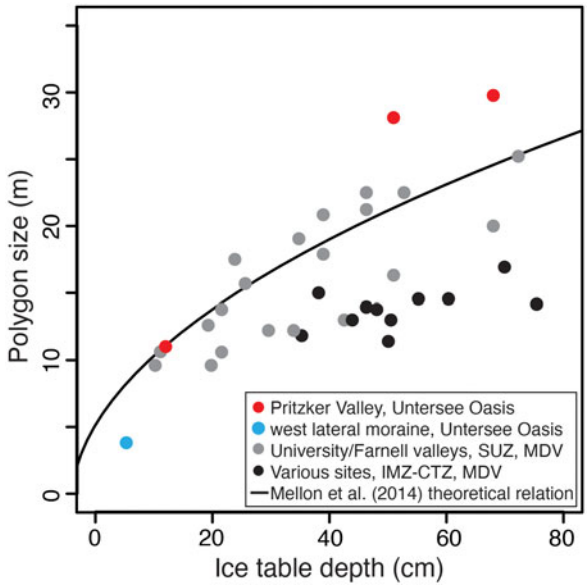

Figure 8. Relation between polygon diameter and ice-table depth in the Untersee Oasis compared with other sites in Antarctica: University and Farnell valleys (Mellon *et al.* 2014) and various McMurdo Dry Valley (MDV) sites, where ice-table depths are obtained from Campbell & Claridge (2023) and average polygon diameter was measured using Lidar data from Fountain *et al.* (2017). The black line is the observed relation between the depth to the ice table and the diameter of polygons following numerical modelling of seasonal stress in permafrost (Mellon *et al.* 2014). CTZ = coastal thaw zone; IMZ = intermediate mixed zone; SUZ = stable upland zone.

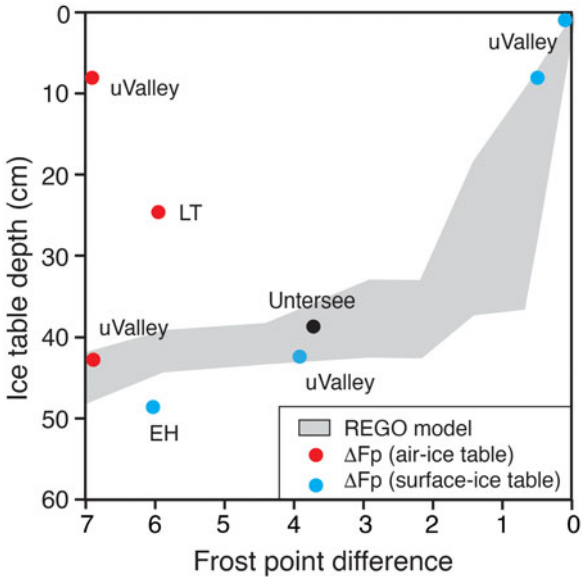

Figure 9. Measured ice-table depths at sites with known frost point differences in the Untersee Oasis, University Valley (uValley), Linneaus Terrace (LT) and Ellsworth Mountains (EH) compared with those predicted by the REGO model (Fisher *et al.* 2016). Table III provides key values of the parameters used in the model.

the air in Antarctica, including the presence of transient snow or frost (McKay 2009, Liu *et al.* 2015, McKay *et al.* 2019). However, the ground surface temperature is cooler than the air from March to October (freezing *nf* are > 1; Fig. 6d), which suggests the absence of snow as an insulating cover (i.e. freezing *nf* are < 1 when snow is present; Smith & Riseborough 1996, 2002). The absence of snow at the sites in the Untersee Oasis is also supported by Sentinel-2 optical images over the period of measurement (appendix A in Gaudreau *et al.* 2024). Generally, terrestrial environments have higher humidity levels at the ground surface than compared to the air (Han *et al.* 2023, Zheng *et al.* 2023). In low-precipitation environments, this observation has been attributed to the hourly temperature variations and cooling of the surface at night, which can result in the formation of dew/frost at the surface that can recharge the soil and reduce soil evaporation. Similarly to non-polar environments, where the formation of early morning dew at the ground surface is influenced by soil moisture, the formation of transient frost in the dry soils above the ice table can help sustain higher ground surface humidity. Numerical modelling by Fisher *et al.* (2016) showed that transient frost accumulates in autumn and winter (cooling seasons) in the dry soils and then ablates in spring and summer (warming seasons). Part of the sublimated transient frost then migrates downward to recharge the ice table, and the remainder migrates towards the surface. This process is reflected in the montly frost point *nf* between the ice table and surface, for which the values progressively increase from February to September (0.6–0.9; Fig. 7d).

Polygon size, depth and source of water for the ice table in Pritzker Valley, Untersee Oasis

In polygons developing in icy permafrost, diurnal and seasonal temperature cycles are the primary drivers of thermal contraction (Lachenbruch 1962). The thermal damping through the dry soil lag sets the temperature at the ice table and the resulting tensile stress: higher stress occurs for shallow ice-table depths, which results in smaller-diameter polygons to relieve the stress. Mellon *et al.* (2014) performed numerical modelling of seasonal stress and strain in icy permafrost and showed that the ice-table depth is a key parameter that controls the diameter of polygons. Much like the polygons in University and Farnell valleys in the upper MDVs (i.e. Mellon *et al.* 2014), the size of the polygons in the Untersee Oasis is also correlated with the depth of the ice table (larger polygons associated with deeper ice tables). In fact, the size and depth of the surveyed polygons align well with the model of Mellon *et al.*

https://doi.org/10.1017/S0954102024000233 Published online by Cambridge University Press

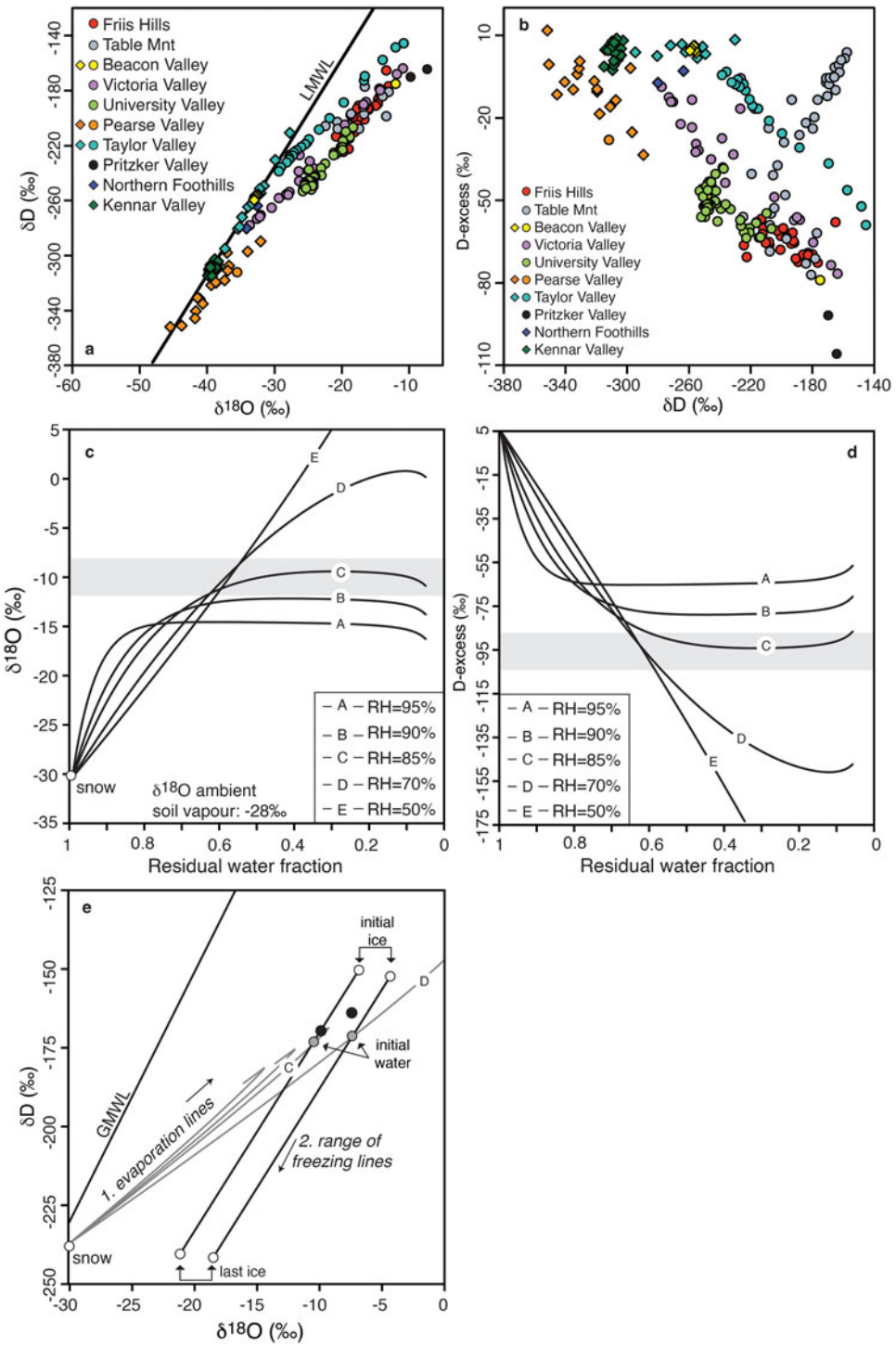

Figure 10. Stable water isotope composition (δD, $\delta^{18}O$ and D-excess) of ground ice in the Untersee Oasis. **a.** δD-$\delta^{18}O$ of ground ice in the Untersee Oasis compared with other sites in the McMurdo Dry Valleys of Antarctica. **b.** D-excess *vs* δD of ground ice in the Untersee Oasis compared with other sites in the McMurdo Dry Valleys of Antarctica. **c. & d.** Evolution of $\delta^{18}O$ and D-excess of evaporating water (1/10th sea water) for a range of relative humidities (RHs) and with an ambient soil water vapour $\delta^{18}O$ of -28‰ using the Criss (1999) and Sofer & Gat (1975) models. The start of snow meltwater is assumed to have $\delta^{18}O$ and δD values of -30.4‰ and -238.2‰, respectively; however, the snow meltwater isotopic composition has a negligible influence on the results. The grey rectangles are the ranges of $\delta^{18}O$ values needed to explain the $\delta^{18}O$ of ground ice at the ice table. **e.** δD-$\delta^{18}O$ of the ground ice at the ice table and the modelled isotope evolution lines for the remaining water for the four scenarios in **c**. A simple Rayleigh freezing model then defines the freezing lines. GMWL = global meteoric water line.

https://doi.org/10.1017/S0954102024000233 Published online by Cambridge University Press

Table III. The values of the variables used in the REGO model. The rheological constants for thermal expansion, creep rates and elasticity are listed in Fisher (2005) and are those that are commonly accepted. Sediment porosity and density values used in the model are similar to the measured values in valleys in the McMurdo Dry Valleys (i.e. McKay *et al.* 1998, Hagedorn *et al.* 2010).

Variable	Value
Dry soil porosity	0.42
Initial ice concentration	385×10^{-7} kg m^{-3}
Density of soil	1300 kg m^{-3}
Temperature (vapour-ice) begins	263 K
Effective diffusivity coefficient of water vapour in air	628 m^2 a^{-1}
Geothermal gradient	+0.02°C m^{-1}
Mean annual ground surface temperature	250 K
Annual temperature amplitude	12°
Daily temperature amplitude	10°
Mean annual relative humidity	50–100‰$_{ice}$
Soil thermal diffusivity	9.5, 36 and 62 m^2 yr^{-1}

(2014); however, some deviations around the theoretical line could be due to the value of the cracking threshold used and to the rheological properties of the icy permafrost (Fig. 8). Overall, the size of polygons and ice-table depths in the Untersee Oasis appear to be in equilibrium.

Studies that have used the air as the boundary layer to evaluate the stability of the ice table suggested that the substantial difference in the frost point between the air (-20.2°C) and ice table (-13.1°C and -11.7°C) should result in the soil column being dry throughout (e.g. McKay *et al.* 1998, Schorghofer 2005, Hagedorn *et al.* 2010, Liu *et al.* 2015). However, the ice-table depths on the Aurkjosen Plateau and Pritzker Valley are < 1 m, and these ice tables are probably in equilibrium with the conditions at the ground surface. Fisher *et al.* (2016) used a numerical model (REGO) to predict the depth of the ice table based on ground surface temperature and humidity as the boundary conditions, along with damping of diurnal and annual temperature cycles within sandy soils. The REGO model predicts that the maximum depth of the ice table is set by the damping depth of the diurnal temperature cycle (50–100 cm for thermal diffusivities between 6 and 62 m^2 yr^{-1}) and the water vapour density gradient between the ground surface and the ice-bearing ground. The measurements from the Untersee Oasis fit well with the predicted ice-table depth for the difference in frost point values between the ground surface and ice table (Fig. 9).

The main source of water that recharges the ice table in Pritzker Valley can be inferred from the δD-δ^{18}O measurements. The δ^{18}O (-9.8‰ and -7.3‰) and D-excess (-91.4‰ and -105.8‰) of ground ice at the ice table at two sites in Pritzker Valley are the highest and lowest values, respectively, reported for ground ice in Antarctica (Fig. 10a,b). The δ^{18}O values approach those of ground ice near the ice table in Victoria Valley (Hagedorn *et al.* 2010), Table Mountain (Dickinson & Rosen 2003) and Friis Hills (Verret *et al.* 2021). Excluding the burial of glacier ice, there are two main mechanisms of ice emplacement in Antarctic permafrost soils: 1) diffusion and deposition of water vapour and 2) episodic freezing of evaporated snow meltwater (e.g. Lacelle *et al.* 2013; Verret *et al.* 2021). The δD-δ^{18}O of ground ice formed from direct condensation of atmospheric moisture in the soils would plot along the LMWL but with D-excess near -35‰; however, if the source of vapour is from transient frost that accumulates in autumn and winter in the dry soils from condensation and then ablates during spring and summer with a portion moving downward to recharge the ice table, the D-excess could reach values near -50‰ (Lacelle *et al.* 2013, Fisher *et al.* 2016, Lapalme *et al.* 2017a). In this environment, while vapor diffusion in soils is a constant process, it accounts for only ~1×10^{-4} g/cc/year of ice formation, requiring ~300–400 years to achieve pore saturation (Lacelle *et al.* 2013; Fisher *et al.* 2016). Given the D-excess values near -100‰, the ground ice at the ice table probably originates from the partial evaporation of snowmelt that infiltrates the dry soil column. This type of ground ice in Antarctic permafrost is usually characterized by high δ^{18}O and δD and very low D-excess, and it has been documented at both the low and high elevations of the MDVs (Dickinson & Rosen 2003, Hagedorn *et al.* 2010, Verret *et al.* 2021). Figure 10c,d shows the evolution of δ^{18}O and D-excess from evaporating snowmelt with an initial δ^{18}O for snow of -30‰, soil water vapour of -28‰ and a range of humidity values followed by freezing of the partially evaporated water based on the models presented in Lapalme *et al.* (2017a), Fisher *et al.* (2020) and Faucher *et al.* (2021a). Although we do not have measurements of the δ^{18}O vapour in soils, the high δ^{18}O values (-9.8‰ and -7.3‰) and D-excess near -100‰ at the ice table can be reached if δ^{18}O soil vapour is in the -30‰ to -20‰ range, soil relative humidity is > 70‰$_{ice}$ and at least 30% of snowmelt evaporates. It is difficult to reach the extremely low D-excess values using an ambient soil humidity equal to that in the atmosphere (~50%; line E in Fig. 10d; i.e. Hagedorn *et al.* 2010). This is an independent corroboration that the ground surface humidity is much higher than that in the air above.

Overall, the depth of the ice table in the Untersee Oasis appears to be controlled by the conditions at the ground surface and the water vapour density gradient between the ground surface and the ice-bearing ground, but it is periodically recharged by the partial evaporation of snowmelt. Using the timing of formation of evaporative calcite crusts in the Untersee Oasis as a proxy of when sufficient snow meltwater is available, a recharge of the

https://doi.org/10.1017/S0954102024000233 Published online by Cambridge University Press

ice table from evaporated snowmelt probably started to occur over the past 2000 years (i.e. Lacelle *et al.* 2024).

Early-stage development of sublimation-type sand-wedge polygons along the western lateral moraine

Sand-wedge polygons that develop following the sublimation of massive ground ice is a special type of feature found only in cold, hyper-arid environments. Currently, they have only been documented in Beacon and Mullins valleys in the stable uplands of the MDVs, where the mean summer air temperature is < 0°C (Marchant *et al.* 2002, Marchant & Head 2007). Their morphology consists of high-centred polygons with diameters in the 9–35 m range, trough depths of 1–3 m and depths to the buried ice of 25–80 cm (Marchant *et al.* 2002). A key characteristic of sublimation-type polygons is their aspect-dependant trough asymmetry (south-facing slopes are steeper than north-facing slopes; Levy *et al.* 2006, 2008). This type of polygon develops high centres because ice exposed by cracking sublimates preferentially. As cracks form, the fine fraction of overlying sediments falls into the crack, creating a sand-wedge, while the coarse fraction remains at the surface and delimits the margins of the polygons.

The sublimation-type polygons in Beacon Valley have arguably been developing for the past 8 Ma. The ones discovered along the western lateral moraine of the Anuchin Glacier in the Untersee Oasis are much younger (Holocene age). Currently, the polygons along the western lateral moraine have small diameters (9–18 m) and very shallow troughs (< 5 cm deep and < 10 cm wide) compared to those in Beacon and Mullins valleys. Over Lake Untersee, the ablation rates of the ice cover are in the order of 0.50–0.75 m yr^{-1} (Faucher *et al.* 2019), but along the western lateral moraine of the Anuchin Glacier, the buried glacial ice is found beneath < 10 cm of dry soils, a depth that is consistent with the ablation of ice beneath a dry lag for < 10 000 years (Fisher *et al.* 2016). The evolution of these polygons will continue to be monitored as they represent early-stage development of sublimation-type sand-wedge polygons.

Conclusions

This study examined the 2019–2023 temperature and humidity conditions, the distribution and development of the polygonal terrain and the origin of ground ice at the ice table in the Untersee Oasis, Antarctica. Based on the results, the following conclusions can be drawn:

1) In the Untersee Oasis, the MAAT ≅ MAGST (surface offset: +0.5°C ± 0.1°C), with the ground surface temperatures being 2–7°C warmer in summer (*nf*: 0.60–0.03) but slightly cooler than the air in winter (*nf*: 1.00–1.06). The MAGST ≤ TTIT (thermal offset: 0.1 and 0.9). These conditions reflect the absence of vegetation and snow and the presence of dry soil above the ice table.
2) The mean annual vapour pressure at the ground surface is ∼2× higher relative to that in the air. The higher vapour pressure at the ground surface is attributed to the formation of transient frost in the dry soils above the ice table, which can help sustain greater ground surface humidity. The process is observable in the monthly frost point *nf* between the ice table and surface, where the values progressively increase from February to September.
3) Polygonal terrain was observed in Pritzker Valley and along the western lateral moraine of the Anuchin Glacier. The sizes of the polygons are positively correlated with the depth of the ice table and align closely with the predictions by Mellon *et al.* (2014). Therefore, the sizes of the polygons are probably in equilibrium with the ice-table depth.
4) The $\delta^{18}O$ (-9.8‰ and -7.3‰) and D-excess (-91.4‰ and -105.8‰) values of ground ice at the ice table in Pritzker Valley suggest that the ice originates from evaporating snowmelt that infiltrated the dry soil column. As such, the depth of the ice table is set by the conditions at the ground surface and the water vapour density gradient between the ground surface and the ice-bearing ground, but it is recharged periodically by the partial evaporation of snowmelt.
5) An early-stage development of sublimation-type sand-wedge polygons was discovered along the western lateral moraine of the Anuchin Glacier in the Untersee Oasis. These have been developing during the Holocene, and they have much smaller diameters (9–18 m) and very shallow troughs (< 5 cm deep and < 10 cm wide) compared to those in the uplands of the MDVs. The buried glacial ice is found beneath < 10 cm of dry soils, a depth that is consistent with the ablation of ice beneath a dry lag for < 10 000 years.
6) Presently, the Untersee Oasis has a local climate that is dominated by intense ablation but with little melt. If warming occurs in the coming decades, this region would be expected to see profound changes in its environment and local landscape, including permafrost. Consequently, there is a need to maintain and expand climate monitoring within the Untersee Oasis, incorporating comprehensive measurements essential for a surface energy balance study, to monitor the resulting impacts on the permafrost environment.

Acknowledgements

This work was supported by the TAWANI Foundation, the Trottier Family Foundation, a NASA Exobiology grant to DTA and a Natural Sciences and Engineering Research

https://doi.org/10.1017/S0954102024000233 Published online by Cambridge University Press

Council of Canada (NSERC) Discovery Grant to DL. Logistical support was provided by the Antarctic Logistics Centre International, Cape Town, South Africa. We thank the two reviewers for their constructive comments.

Competing interests

The authors declare none.

Author contributions

All authors designed the project; all authors contributed to data collection; all authors contributed to data analysis and writing the manuscript.

References

Adlam, L.S., Balks, M.R., Seybold, C.A. & Campbell, D.I. 2010. Temporal and spatial variation in active layer depth in the McMurdo Sound Region, Antarctica. *Antarctic Science*, **22**, 10.1017/S0954102009990460.

Andersen, D.T., McKay, C.P. & Lagun, V. 2015. Climate conditions at perennially ice-covered Lake Untersee, East Antarctica. *Journal of Applied Meteorology and Climatology*, **54**, 10.1175/JAMC-D-14-0251.1.

Bockheim, J.G. 2015. Soil-forming factors in Antarctica. *In* Bockheim, J.G., *ed*., *The soils of Antarctica*. Cham: Springer, 10.1007/978-3-319-05497-1_2.

Bockheim, J.G., Campbell, I.B. & McLeod, M. 2007. Permafrost distribution and active-layer depths in the McMurdo Dry Valleys, Antarctica. *Permafrost and Periglacial Processes*, **18**, 10.1002/ppp.588.

Bockheim, J.G., Vieira, G., Ramos, M., López-Martínez, J., Serrano, E., Guglielmin, M., *et al*. 2013. Climate warming and permafrost dynamics in the Antarctic Peninsula region. *Global and Planetary Change*, **100**, 10.1016/J.GLOPLACHA.2012.10.018.

Bormann, P., Bankwitz, P., Bankwitz, E., Damn, V., Hurtig, E., Kampf, H., *et al*. 1986. Structure and development of the passive continental margin across the Princess Astrid Coast, East Antarctica. *Journal of Geodynamics*, **373**, 347–373.

Brooks, S.T., Jabour, J., van den Hoff, J. & Bergstrom, D.M. 2019. Our footprint on Antarctica competes with nature for rare ice-free land. *Nature Sustainability*, **2**, 10.1038/s41893-019-0237-y.

Campbell, I.B. & Claridge, G.G. 2023. *Manaaki Whenua - Landcare Research Report*. 1964-1999 *Ross Sea region soils.* Available at https://antarctic-soils.landcareresearch.co.nz/

Cannone, N. & Guglielmin, M. 2009. Influence of vegetation on the ground thermal regime in continental Antarctica. *Geoderma*, **151**, 10.1016/J.GEODERMA.2009.04.007.

Criss, R.E. 1999. *Principles of stable isotope distribution*. Oxford: Oxford University Press, 268 pp.

Dickinson, W.W. & Rosen, M.R. 2003. Antarctic permafrost: an analogue for water and diagenetic minerals on Mars. *Geology*, **31**, 10.1130/0091-7613(2003)031<0199:APAAFW>2.0.CO;2.

Eaton, A.K., Rouse, W.R., Lafleur, P.M., Marsh, P. & Blanken, P.D. 2001. Surface energy balance of the western and central Canadian subarctic: variations in the energy balance among five major terrain types. *Journal of Climate*, **14**, 10.1175/1520-0442(2001)014.

Faucher, B., Lacelle, D., Fisher, D.A., Andersen, D.T. & McKay, C.P. 2019. Energy and water mass balance of Lake Untersee and its perennial ice cover, East Antarctica. *Antarctic Science*, **31**, 10.1017/S0954102019000270.

Faucher, B., Lacelle, D., Marsh, N.B., Fisher, D.A. & Andersen, D.T. 2021a. Ice-covered ponds in the Untersee Oasis (East Antarctica): distribution, chemical composition, and trajectory under a warming climate. *Arctic, Antarctic, and Alpine Research*, **53**, 10.1080/15230430.2021.2000566.

Faucher, B., Lacelle, D., Davila, A., Pollard, W., Fisher, D. & McKay, C.P. 2017. Physicochemical and biological controls on carbon and nitrogen in permafrost from an ultraxerous environment, McMurdo Dry Valleys of Antarctica. *Journal of Geophysical Research - Biogeosciences*, **122**, 10.1002/2017JG004006.

Faucher, B., Lacelle, D., Marsh, N.B., Jasperse, L., Clark, I.D. & Andersen, D.T. 2021b. Glacial lake outburst floods enhance benthic microbial productivity in perennially ice-covered Lake Untersee (East Antarctica). *Communications Earth & Environment* **2**, 10.1038/s43247-021-00280-x.

Fisher, D.A. 2005. A process to make massive ice in the Martian regolith using long-term diffusion and thermal cracking. *Icarus*, **179**, 387–397.

Fisher, D.A., Lacelle, D., Pollard, W. & Faucher, B. 2020. A model for stable isotopes of residual liquid water and ground ice in permafrost soils using arbitrary water chemistries and soil-specific empirical residual water functions. *Permafrost and Periglacial Processes*, **32**, 10.1002/ppp.2079.

Fisher, D.A., Lacelle, D., Pollard, W., Davila, A.F. & McKay, C.P. 2016. Ground surface temperature and humidity, ground temperature cycles and the ice table depths in University Valley, McMurdo Dry Valleys of Antarctica. *Journal of Geophysical Research - Earth Surface*, **121**, 10.1002/2016JF004054.

Fountain, A.G., Nylen, T.H., Monaghan, A., Basagic, H.J. & Bromwich, D. 2010. Snow in the McMurdo Dry Valleys, Antarctica. *International Journal of Climatology*, **30**, 10.1002/joc.1933.

Gardner, C.B., Diaz, M.A., Smith, D.F., Fountain, A.G., Levy, J.S. & Lyons, W.B. 2022. Isotopic signature of massive, buried ice in eastern Taylor Valley, Antarctica: implications for its origin. *Arctic, Antarctic, and Alpine Research*, **54**, 10.1080/15230430.2022.2102510.

Gaudreau, A., Lacelle, D. & Andersen, D.T. 2024. Synthetic aperture radar backscatter is influenced by bubbles at the ice/water interface of an Antarctic lake. *Communications Earth & Environment* **5**, 10.1038/S43247-024-01370-2.

Goordial, J., Davila, A.F., Lacelle, D., Pollard, W., Marinova, M.M., Greer, C.W., *et al*. 2016. Nearing the cold-arid limits of microbial life in permafrost of an upper dry valley, Antarctica. *ISME Journal*, **10**, 10.1038/ismej.2015.239.

Guglielmin, M., Dalle Fratte, M. & Cannone, N. 2014. Permafrost warming and vegetation changes in Continental Antarctica. *Environmental Research Letters*, **9**, 10.1088/1748-9326/9/4/045001.

Hagedorn, B., Sletten, R.S. & Hallet, B. 2007. Sublimation and ice condensation in hyperarid soils: modeling results using field data from Victoria Valley, Antarctica. *Journal of Geophysical Research*, **112**, 10.1029/2006JF000580.

Hagedorn, B., Sletten, R.S., Hallet, B., McTigue, D.F. & Steig, E.J. 2010. Ground ice recharge via brine transport in frozen soils of Victoria Valley, Antarctica: insights from modeling $\delta^{18}O$ and δD profiles. *Geochimica et Cosmochimica Acta*, **74**, 10.1016/J.GCA.2009.10.021.

Han, Q., Zeng, Y., Zhang, L., Wang, C., Prikaziuk, E., Niu, Z. & Su, B. 2023. Global long term daily 1 km surface soil moisture dataset with physics informed machine learning. *Scientific Data* **10**, 10.1038/s41597-023-02011-7.

Hiller, A., Wand, U., Kämpf, H. & Stackebrandt, W. 1988. Occupation of the Antarctic continent by petrels during the past 35 000 years: inferences from a ^{14}C study of stomach oil deposits. *Polar Biology*, **9**, 10.1007/BF00442032.

Hoffman, M.J., Fountain, A.G. & Liston, G.E. 2008. Surface energy balance and melt thresholds over 11 years at Taylor Glacier, Antarctica. *Journal of Geophysical Research - Earth Surface*, **113**, 10.1029/2008JF001029.

Hrbáček, F., Oliva, M., Hansen, C., Balks, M., O'Neill, T.A., de Pablo, M.A., *et al*. 2023. Active layer and permafrost thermal regimes in the ice-free areas of Antarctica. *Earth-Science Reviews*, **242**, 10.1016/J.EARSCIREV.2023.104458.

Hrbáček, F., Vieira, G., Oliva, M., Balks, M., Guglielmin, M., de Pablo, M.Á., *et al*. 2021. Active layer monitoring in Antarctica: an overview of results from 2006 to 2015. *Polar Geography*, **44**, 10.1080/1088937X.2017.1420105.

Kampf, H. & Stakerbrandt, W. 1985. Geological investigation in the Eliseev anorthosite massif, central Dronning Maud Land, East Antarctica. *Zeitschrift fur. Geologische Wissenschaften*, **13**, 32–60.

Karunaratne, K.C. & Burn, C.R. 2004. Relations between air and surface temperature in discontinuous permafrost terrain near Mayo, Yukon Territory. *Canadian Journal of Earth Sciences*, **41**, 10.1139/e04-082.

Klene, A.E., Nelson, F.E., Shiklomanov, N.I., Hinkel, K.M., Klene, A.E., Nelson, F.E., *et al*. 2001. The N-factor in natural landscapes: variability of air and soil-surface temperatures, Kuparuk River Basin, Alaska, U.S.A. *Arctic Antarctic and Alpine Research*, **33**, 140–148.

Kotzé, C. & Meiklejohn, I. 2017. Temporal variability of ground thermal regimes on the northern buttress of the Vesleskarvet nunatak, western Dronning Maud Land, Antarctica. *Antarctic Science*, **29**, 10.1017/S095410201600047X.

Lacelle, D., Christy, M., Faucher, B., Sobron, P. & Andersen, D. 2024. Palaeo-environmental significance of evaporative calcite crusts in the Untersee Oasis, East Antarctica. *Antarctic Science*, 10.1017/S0954102024000075.

Lacelle, D., Lapalme, C.M., Davila, A.F., Pollard, W., Marinova, M., Heldmann, J. & McKay, C.P. 2016. Solar radiation and air and ground temperature relations in the cold and hyper-arid Quartermain Mountains, McMurdo Dry Valleys of Antarctica. *Permafrost and Periglacial Processes*, **27**, 10.1002/ppp.1859.

Lacelle, D., Davila, A.F., Fisher, D., Pollard, W.H., DeWitt, R., Heldmann, J., *et al*. 2013. Excess ground ice of condensation-diffusion origin in University Valley, Dry Valleys of Antarctica: evidence from isotope geochemistry and numerical modeling. *Geochimica et Cosmochimica Acta*, **120**, 10.1016/j.gca.2013.06.032.

Lachenbruch, A.H. 1962. Mechanics of thermal contraction cracks and ice-wedge polygons in permafrost. *Geological Society of America Special Papers*, **70**, 10.1016/0378-7788(86)90031-9.

Lapalme, C.M., Lacelle, D., Pollard, W., Fisher, D., Davila, A. & McKay, C.P. 2017a. Distribution and origin of ground ice in University Valley, McMurdo Dry Valleys, Antarctica. *Antarctic Science*, **29**, 10.1017/S0954102016000572.

Lapalme, C.M., Lacelle, D., Pollard, W., Fortier, D., Davila, A. & McKay, C.P. 2017b. Cryostratigraphy and the sublimation unconformity in permafrost from an ultraxerous environment, University Valley, McMurdo Dry Valleys of Antarctica. *Permafrost and Periglacial Processes*, **28**, 10.1002/ppp.1948.

Levy, J.S., Marchant, D.R. & Head, J.W. 2006. Distribution and origin of patterned ground on Mullins Valley debris-covered glacier, Antarctica: the roles of ice flow and sublimation. *Antarctic Science*, **18**, 10.1017/S0954102006000435.

Levy, J.S., Head, J.W., Marchant, D.R. & Kowalewski, D.E. 2008. Identification of sublimation-type thermal contraction crack polygons at the proposed NASA Phoenix landing site: implications for substrate properties and climate-driven morphological evolution. *Geophysical Research Letters*, **35**, 10.1029/2007GL032813.

Levy, J.S., Fountain, A.G., Gooseff, M.N., Welch, K.A. & Lyons, W.B. 2011. Water tracks and permafrost in Taylor Valley, Antarctica: extensive and shallow groundwater connectivity in a cold desert ecosystem. *GSA Bulletin*, **123**, 10.1130/B30436.1.

Liu, L., Sletten, R.S., Hagedorn, B., Hallet, B., McKay, C.P. & Stone, J.O. 2015. An enhanced model of the contemporary and long-term (200 ka) sublimation of the massive subsurface ice in Beacon Valley, Antarctica. *Journal of Geophysical Research - Earth Surface*, **120**, 10.1002/2014JF003415.

Marchant, D.R. & Head, J.W. 2007. Antarctic dry valleys: microclimate zonation, variable geomorphic processes, and implications for assessing climate change on Mars. *Icarus*, **192**, 10.1016/j.icarus.2007.06.018.

Marchant, D.R., Lewis, A.R., Phillips, W.M., Moore, E.J., Souchez, R.A., Denton, G.H., *et al*. 2002. Formation of patterned ground and sublimation till over Miocene glacier ice in Beacon Valley, southern Victoria Land, Antarctica. *Geological Society of America Bulletin*, **114**, 10.1130/0016-7606(2002)114<0718:FOPGAS>2.0.CO;2.

Marinova, M.M., McKay, C.P., Heldmann, J.L., Goordial, J., Lacelle, D., Pollard, W.H. & Davila, A.F. 2022. Climate and energy balance of the ground in University Valley, Antarctica. *Antarctic Science*, **34**, 10.1017/S0954102022000025.

McKay, C.P. 2009. Snow recurrence sets the depth of dry permafrost at high elevations in the McMurdo Dry Valleys of Antarctica. *Antarctic Science*, **21**, 10.1017/S0954102008001508.

McKay, C.P., Mellon, M.T. & Friedmann, E.I. 1998. Soil temperatures and stability of ice-cemented ground in the McMurdo Dry Valleys, Antarctica. *Antarctic Science*, **10**, 10.1017/S0954102098000054.

McKay, C.P., Balaban, E., Abrahams, S. & Lewis, N. 2019. Dry permafrost over ice-cemented ground at Elephant Head, Ellsworth Land, Antarctica. *Antarctic Science*, **31**, 10.1017/S0954102019000269.

Mellon, M.T., McKay, C.P. & Heldmann, J.L. 2014. Polygonal ground in the McMurdo Dry Valleys of Antarctica and its relationship to ice-table depth and the recent Antarctic climate history. *Antarctic Science*, **26**, 10.1017/S0954102013000710.

Obryk, M.K., Doran, P.T., Fountain, A.G., Myers, M. & McKay, C.P. 2020. Climate from the McMurdo Dry Valleys, Antarctica, 1986–2017: surface air temperature trends and redefined summer season. *Journal of Geophysical Research - Atmospheres*, **125**, 10.1029/2019JD032180.

Obu, J., Westermann, S., Vieira, G., Abramov, A., Ruby Balks, M., Bartsch, A., *et al*. 2020. Pan-Antarctic map of near-surface permafrost temperatures at 1km^2 scale. *Cryosphere*, **14**, 10.5194/TC-14-497-2020.

Paech, H.-J. & Stackebrandt, W. 1995. Geology. *In* Bormann, P. & Fritzsche, D., *eds*, *The Schirmacher Oasis, Queen Maud Land, East Antarctica and its surroundings*. Cambridge, Cambridge University Press, 59–159.

Pringle, D.J., Dickinson, W.W., Trodahl, H.J. & Pyne, A.R. 2003. Depth and seasonal variations in the thermal properties of Antarctic Dry Valley permafrost from temperature time series analysis. *Journal of Geophysical Research - Solid Earth*, **108**, 10.1029/2002JB002364.

Schorghofer, N. 2005. A physical mechanism for long-term survival of ground ice in Beacon Valley, Antarctica. *Geophysical Research Letters*, **32**, 10.1029/2005GL023881.

Schwab, M.J. 1998. *Reconstruction of the late Quaternary climatic and environmental history of the Schirmacher Oasis and the Wohlthat Massif* (*east Antarctica*). Bremerhaven: Alfred-Wegener-Institut für Polar- und Meeresforschung, 128 pp.

Schwerdtfeger, W. 1984. Weather and climate of the Antarctic. *Developments in Atmospheric Science*, **15**, 10.2307/633555.

Shamilishvili, G., Abakumov, E.V. & Andersen, D. 2020. Biogenic-abiogenic interactions and soil formation in extreme conditions of Untersee Oasis, surroundings of Lake Untersee, central Queen Maud Land, East Antarctica. *In* Frank-Kamenetskaya, O., Vlasov, D., Panova, E. & Lessovaia, S., *eds*, *Processes and phenomena on the boundary between biogenic and abiogenic nature*. Lecture Notes in Earth System Sciences. Cham: Springer, 10.1007/978-3-030-21614-6_25/TABLES/4.

Smith, M.W. & Riseborough, D.W. 1996. Permafrost monitoring and detection of climate change. *Permafrost and Periglacial Processes*, **7**, 10.1002/(SICI)1099-1530(199610)7:4<301::AID-PPP231>3.0.CO;2-R.

Smith, M.W. & Riseborough, D.W. 2002. Climate and the limits of permafrost: a zonal analysis. *Permafrost and Periglacial Processes*, **13**, 10.1002/PPP.410.

Sofer, Z. & Gat, J.R. 1975. The isotope composition of evaporating brines: effect of the isotopic activity ratio in saline solutions. *Earth and Planetary Science Letters*, **26**, 10.1016/0012-821X(75)90085-0.

Swanger, K.M. 2017. Buried ice in Kennar Valley: a late Pleistocene remnant of Taylor Glacier. *Antarctic Science*, **29**, 10.1017/S0954102016000687.

Swanger, K.M., Marchant, D.R., Kowalewski, D.E. & Head, J.W. 2010. Viscous flow lobes in central Taylor Valley, Antarctica: origin as remnant buried glacial ice. *Geomorphology*, **120**, 10.1016/j.geomorph.2010.03.024.

Van den Broeke, M., van de Berg, W., van Meijgaard, E. & Reijmer, C. 2006. Identification of Antarctic ablation areas using a regional atmospheric climate model. *Journal of Geophysical Research - Atmospheres*, **111**, 10.1029/2006JD007127.

Van Wessem, J.M., Ligtenberg, S.R.M., Reijmer, C.H., Van De Berg, W.J., Van Den Broeke, M.R., Barrand, N.E., *et al*. 2016. The modelled surface mass balance of the Antarctic Peninsula at 5.5-km horizontal resolution. *Cryosphere*, **10**, 10.5194/TC-10-271-2016.

Verret, M., Dickinson, W., Lacelle, D., Fisher, D., Norton, K., Chorley, H., *et al*. 2021. Cryostratigraphy of mid-Miocene permafrost at Friis Hills, McMurdo Dry Valleys of Antarctica. *Antarctic Science*, **33**, 10.1017/S0954102020000619.

Vieira, G., Bockheim, J.G., Guglielmin, M., Balks, M., Abramov, A.A., Boelhouwers, J., *et al*. 2010. Thermal state of permafrost and active-layer monitoring in the Antarctic: advances during the international polar year 2007–2009. *Permafrost and Periglacial Processes*, **21**, 10.1002/ppp.685.

Zheng, C., Jia, L. & Zhao, T. 2023. A 21-year dataset (2000–2020) of gap-free global daily surface soil moisture at 1-km grid resolution. *Scientific Data*, **10**, 10.1038/s41597-023-01991-w.